Journal of Materials Chemistry C

Accepted Manuscript

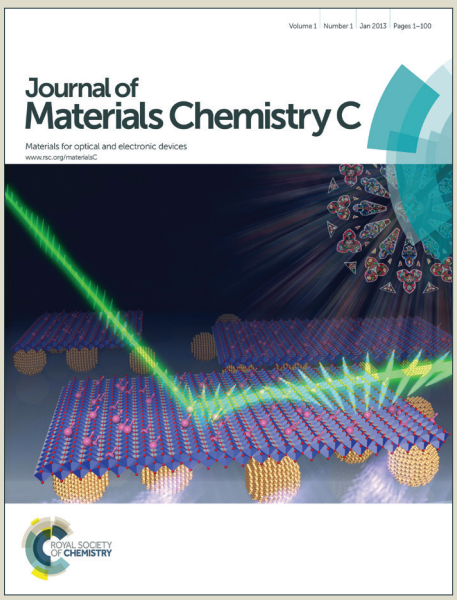

ROYAL SOCIETY OF CHEMISTRY

www.rsc.org/materialsC

UV-Induced Improvement in ZnO Thin Film Conductivity: A New *in situ* Approach

Authors:

Alex T. Vai, Vladimir L. Kuznetsov, Jonathan R. Dilworth, Peter P. Edwards*

Inorganic Chemistry Laboratory, Department of Chemistry, University of Oxford, South Parks Road, OXFORD OX1 3QR, UK
* To whom correspondence should be addressed: peter.edwards@chem.ox.ac.uk

Abstract:

We report a long-lasting enhancement in electrical properties occurs when zinc oxide (ZnO) thin films prepared by spray pyrolysis in a nitrogen atmosphere are treated with UV prior to the films' first exposure to air (here termed "*in situ* irradiation"). Carrier mobilities as high as 44.3 cm^2/Vs – the highest values yet reported for any ZnO thin films made by spray pyrolysis – are exhibited by samples deposited at *ca.* 376 °C. In fact, such mobility values compare favorably with results that have been obtained using more complex, vacuum-based deposition techniques. The results of electrical, chemical, and microstructural characterization as a function of irradiation and deposition temperature indicate that the improved electrical properties stem from a modification of the relative populations of donor and acceptor defects at the grain boundaries of these polycrystalline films, allowing parallels to be drawn to the well-known phenomenon of "persistent" photoconductivity in ZnO. Finally, we consider how these observations about the interaction of ZnO with UV light relate to factors that limit the electrical performance of practical, transparent conducing oxide thin films.

Introduction:

The combination of properties that define transparent conducting oxides (TCOs) – simultaneous transparency to visible light and highly tunable electrical conductivity – enable a range of technologies that are essential to the modern world. As thin films, TCOs are used as transparent electrodes in electronic displays, touchscreen sensors, and photovoltaic cells, as the semiconducting channel layer in transparent thin-film transistors (TFTs), and as low emissivity coatings on glass for a range of architectural and household applications.[1, 2] Taken in sum, the demand for these

applications leads to a market for transparent conductors worth well over 1.5 billion US Dollars per year.[3]

The electrical and optical performance of a TCO film is most directly related to its carrier concentration (n) and its carrier mobility (μ). These two parameters come together to determine the electrical conductivity (σ) according to the relation $\sigma = ne\mu$, where e is the elementary charge.[4] It is always important to realize that optimal values for n and μ can vary dramatically depending on the particular application for which a TCO film is intended.[5] As two contrasting examples, low emissivity glass coatings require films with a high enough n to result in high infrared reflectivity, whereas transparent TFTs explicitly require a transparent channel layer with high μ, but low n.

As a prototypical n-type TCO, zinc oxide (ZnO) has attracted a great deal of research and commercial attention because of its high earth-abundance, extremely low cost, and suitability for deposition using scalable, solution-based techniques like spray pyrolysis.[6-8] For the TCO applications where the performance of ZnO is adequate, these positive attributes represent compelling advantages over the indium oxide-based materials (especially ITO) that currently make up a majority of the value in the global transparent conductor market.[9-11] At present, a major research challenge is to better understand – and ultimately overcome – factors limiting the electrical performance of ZnO-based materials prepared using commercially-relevant techniques, so as to increase the number of applications in which it can successfully replace ITO.

The fact that ZnO – both in the bulk and as a thin film – is excited and activated by light is well established. Of particular interest have been photoconductive effects, where the electrical conductivity of ZnO changes upon irradiation. These types of effects have been exploited in a variety of sensing applications[12-14] and to activate nanoparticle ZnO catalysts for the photodegradation of organics.[15, 16] The most studied of these effects in ZnO has been so-called "persistent" photoconductivity, which is distinguished by the fact that its effects decay only over a timescale of hours to days when a sample that has been irradiated is stored in air.[17]

We report here a new and even longer-lived photoconductive effect in polycrystalline ZnO films deposited by spray pyrolysis under nitrogen, which arises as a result of UV irradiation of the films before they are first exposed to air. Using this approach, films with Hall effect mobility of up to 44.3 cm^2/Vs have been prepared at a substrate temperature of 376 °C. To our knowledge, this is the highest mobility yet reported for ZnO films deposited by spray pyrolysis and compares very well with the mobilities in films deposited with industry-standard vacuum sputtering techniques.[18] In addition, an average conductivity of 13.3 ± 3.0 $\Omega^{-1}cm^{-1}$ was achieved at 334 °C. This is a much lower deposition temperature than that required to prepare the most conductive undoped ZnO films by spray pyrolysis in the absence of irradiation. Such a reduction in processing temperature could also facilitate the emergence of transparent conductor applications using flexible, temperature-sensitive substrates.[19, 20]

We have applied a variety of electrical, chemical, and structural characterization techniques to examine the nature of this new, long-lasting photoconductive effect and its relationship with classic "persistent" photoconductivity. The results indicate that despite significant mechanistic parallels, these two phenomena largely act independently of each other, and have a dominating effect on electrical properties of films deposited at higher and lower temperatures, respectively. We also discuss how these observations provide specific insights into the factors that limit the performance of practical ZnO TCO thin films, and may inform ongoing efforts to expand the applicability of low-cost TCO materials and deposition techniques.

Experimental:

Film Deposition

The spray pyrolysis procedure, apparatus, and zinc acetate precursor solutions used to prepare the ZnO films are as previously described.[21] Thermal feedback from the system is taken from the center of the heater block. However, the reported deposition temperatures are of the substrate surface, based on a series of calibration measurements using an optical pyrometer. Temperature uniformity across the substrate surface was approximately ± 7 °C.

For depositions in the dark, precautions were taken to exclude ambient light from the spray chamber. For depositions with *in situ* irradiation, a modified chamber front with a 65 mm diameter fused quartz window was used to permit the UV irradiation of the film inside the chamber. A UVP EL Series blacklight with emission centered at 365 nm (3.4 eV) illuminated the film at an angle of 45° and at a distance of 10 cm, resulting in a total radiative flux of ~140 μW/cm^2 as measured by a Newport 842-PE power/energy meter. Unless otherwise noted, the light source was on from the end of solution spraying until just before the chamber was opened to ambient atmosphere at a heater temperature of less than 50 °C.

Film Characterization

Temperature dependent electrical transport properties of the films were analysed by the van der Pauw method[22] using an Ecopia HMS-3000 Hall effect measurement system with a 0.55 T permanent magnet. Indium solder was used to create four Ohmic electrical contacts on the corners of a 7 mm × 7mm piece of film. For samples deposited at lower heater temperatures that were not of sufficient conductivity to allow reliable carrier concentration and mobility measurements, only electrical resistivity is reported. Measurements at temperatures below (to ~80 K) and above (to ~350 K) ambient temperature were achieved using a custom-designed heating and cooling system. Sample temperature was measured with a Type T thermocouple embedded in the sample mount and in contact with the film substrate.

For Hall effect measurements after *ex situ* irradiation, film pieces were mounted to a sample holder and irradiated with the 365 nm EL Series blacklight from a distance of ~10 cm until a multimeter showed the sample was at constant resistance (after about 5 minutes). The samples were then quickly loaded into the HMS-3000, with measurements being taken within 15 seconds of the sample being removed from the light. For real-time monitoring of *ex situ* photoconductivity, a ZnO thin film sample previously stored in the dark for several days was mounted to a custom circuit board providing connection points for a 2-point resistance measurement and that could be enclosed in a plastic chamber with Luer ports for the supply of various gases (dry nitrogen, nitrogen passed

through a water bubbler, and compressed air). An Agilent 34401A Digital Multimeter was used to measure and record the resistance of the sample before, during, and after irradiation by the 365 nm EL Series blacklight while a chosen gas was flowed over the sample at a rate of ~15 L min^{-1}.

Optical transmission measurements were made for wavelengths between 320 and 2000 nm using a Perkin-Elmer Lambda19 UV-Vis-NIR spectrophotometer. Film thicknesses and transparencies were estimated from this data using the envelope method of Swanepoel.[23]

The surface morphology of the thin films was characterized using a JEOL JSM-840F field emission scanning electron microscope at an accelerating voltage of 5 kV. Samples were sputter coated with a ~2.5 nm layer of platinum before observation in the SEM to reduce the effect of surface charging and attendant artefacts.

X-ray diffraction measurement of samples was performed using a PANalytical X'Pert PRO diffractometer with a Bragg-Brentano geometry and a fixed X-ray source at an emission current of 40 mA and an anode voltage of 45 kV. The spectra were recorded using monochromated Cu-$K_{\alpha 1}$ (λ = 1.5406 Å) or Cu-K_{α} (λ = 1.5418 Å) radiation over a time of 115 minutes. Samples were placed on a 60 rpm spinner to improve averaging of crystallite orientation.

X-ray photoelectron spectroscopy (XPS) was carried out at the National EPSRC XPS User's service (NEXUS) located at Newcastle University (Newcastle upon Tyne, UK) using an AXIS NOVA (Kratos Analytical, Manchester, UK) instrument with an Al K_{α} x-ray source (1486.6 eV). Thin film samples that had been previously exposed to air were analysed without any pre-treatment. Spectra were collected with 20 eV pass energy and 10 sweeps. Low energy electrons were directed at the surface throughout analysis for charge neutralization. For energy calibration, the main peak in the C(1s) spectra (resulting from adventitious surface carbon) was referenced to a binding energy of 285 eV; all other spectra from the same sample were shifted accordingly. The CasaXPS software suite was used for data analysis and fitting. The O(1s) spectra were fitted using a Shirley background, and with components constrained to have the same FWHM and a GL(30) lineshape.

Results:

When undoped ZnO thin films prepared by spray pyrolysis are exposed to UV with energy exceeding that of its electronic bandgap (~3.4 eV) before the films are first removed from the N_2-filled deposition chamber (which we term "*in situ* irradiation", Figure 1b), an increase in electrical conductivity is observed compared to films deposited in the dark (Figure 2). The relative improvement in electrical conductivity consistently increases with decreasing deposition temperature, even though the absolute electrical performance decreases sharply for substrate surface temperatures below 334 °C. The electrical conductivities of films deposited using *in situ* irradiation are similar for deposition temperatures of 334 °C or greater, with the highest average conductivity of 13.3 ± 3.0 Ω^{-1} cm^{-1} achieved at 334 °C. Considering that the maximum conductivity for films deposited in the dark is 8.9 ± 1.3 Ω^{-1} cm^{-1} for films deposited at 417 °C, *in situ* irradiation effectively reduces the maximum processing temperature needed to produce undoped ZnO films with the highest electrical conductivity by over 80 °C.

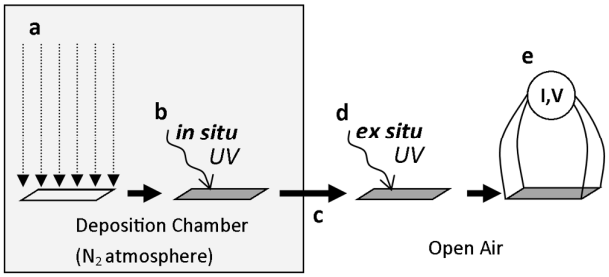

Figure 1 Scheme showing the preparation, *in situ* and *ex situ* UV treatment, and characterization steps for the ZnO thin films in this study. In a nitrogen-filled deposition chamber, a zinc acetate precursor solution is decomposed by intereaction with a heated substrate to form a ZnO thin film (a). After deposition, the film may be irradiated with UV *in situ* while it remains under the inert atmosphere of the deposition chamber (b). Once the sample is removed from the chamber and initially exposed to air (c), an optional *ex situ* UV irradiation (d) of the film can be performed just prior to electrical characterization of the sample (e). Depending on the situation, steps (b) and/or (d) may be omitted.

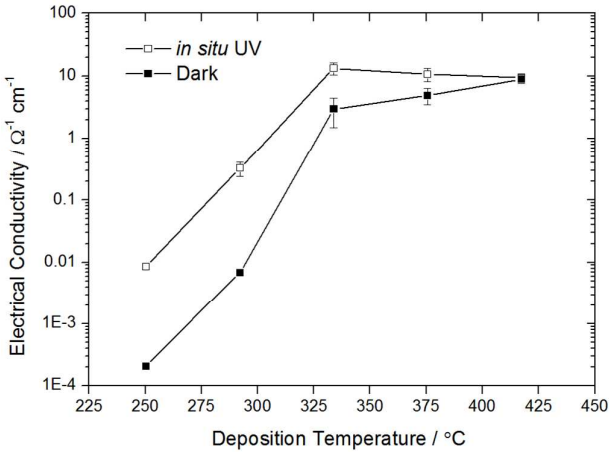

Figure 2 Electrical conductivity of undoped ZnO thin films as a function of deposition temperature for films deposited in the dark (filled symbols) and with *in situ* UV irradiation (open symbols). Where shown, error bars represent the standard deviation in the population of samples deposited under the same conditions. The lowest temperature pair of data points are estimates based on 2-point resistance measurements since these samples were too resistive to be accurately measured using a van der Pauw geometery.

For the films deposited at 334 °C and above, the electrical conductivity increase from *in situ* treatment is considerably longer lived than that seen in previous reports of ZnO photoconductivity, remaining largely unchanged even if the samples are stored in open air for several months. Repeated measurements of the electrical conductivity at different times after deposition are presented in Figure 3 for a sample deposited at 376 °C. The small variability in the conductivity with time can likely be ascribed to classic photoconductive effects, as the ambient lighting conditions before and during resistivity measurements were not strictly controlled. In contrast, the improvement in electrical conductivity resulting from *ex situ* UV irradiation – i.e., after the initial exposure of a film to air – is clearly temporary (Figure 4). When irradiation occurs while a film is exposed to flowing air, the photoconductivity decays more than an order of magnitude within one hour of the irradiation ceasing. Even when *ex situ* irradiation occurs under flowing nitrogen, noticeable decay can be observed over the timescale of a day.

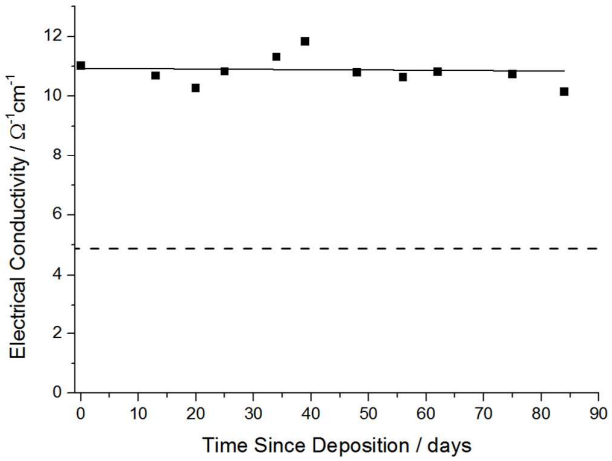

Figure 3 Electrical conductivity of ZnO thin film deposited at 376 °C as a function of time since deposition with *in situ* UV irradiation. The data (with linear trendline) shows the persistence of the effect when the film is stored in air. The dashed line indicates the average electrical conductivity of films deposited in the dark under the same conditions.

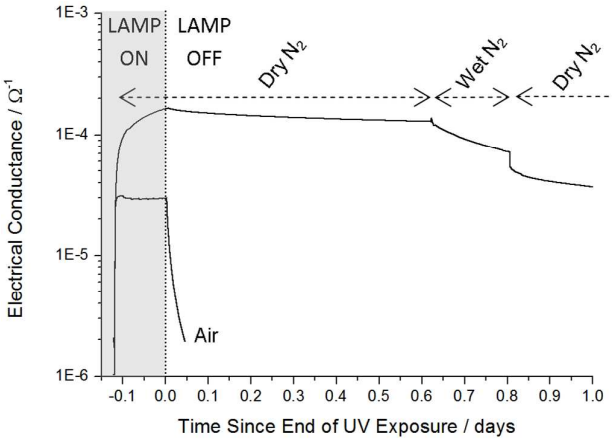

Figure 4 Electrical conductance of ZnO film deposited at 292 °C during (shaded region) and after *ex situ* irradiation under various flowing gases. The zero of time marks the point at which the UV irradiation was stopped. The conductance of the sample after being stored in the dark for two days was $< 5 \times 10^{-10}$ Ω^{-1}.

Room temperature Hall effect measurements to determine the carrier concentration and mobility were carried out on all samples with high enough conductivity for reliable measurements. A listing of all samples and their electrical properties is provided in the Electronic Supplementary Information. Where shown, error bars in the following figures depict the standard deviation in a given property over the population of films deposited under the same conditions. The Hall carrier mobility for films deposited at various temperatures and measured directly after removal from the deposition chamber is shown in Figure 5a. *In situ* irradiation leads to a statistically significant improvement in Hall mobility at all deposition temperatures for which a direct comparison is available. The largest absolute improvement in mobility occurs for films deposited at 376 °C, at which temperature a maximum carrier mobility value of 44.3 cm^2/Vs was achieved (the average over

18 samples was 37.4 ± 3.5 cm^2/Vs). This is a 86% (>4 standard deviation) improvement compared to films deposited in the dark at the same temperature. For both irradiated and dark cases, carrier mobility is strongly dependent on deposition temperature, with all films deposited at 292 °C or lower having a carrier mobility less than 1 cm^2/Vs, which was the lower limit for reliable measurements with available equipment.

The corresponding carrier concentration data is shown in Figure 5b. For films deposited at 334 °C, *in situ* irradiation results in an approximate doubling of the carrier concentration relative to both higher temperature films and films deposited in the dark at the same temperature. This increase in carrier concentration is in addition to a substantial mobility enhancement. It is this higher carrier concentration that allows *in situ* irradiated films deposited at 334 °C to have a similar conductivity as films deposited at higher temperatures, despite having a somewhat lower carrier mobility.

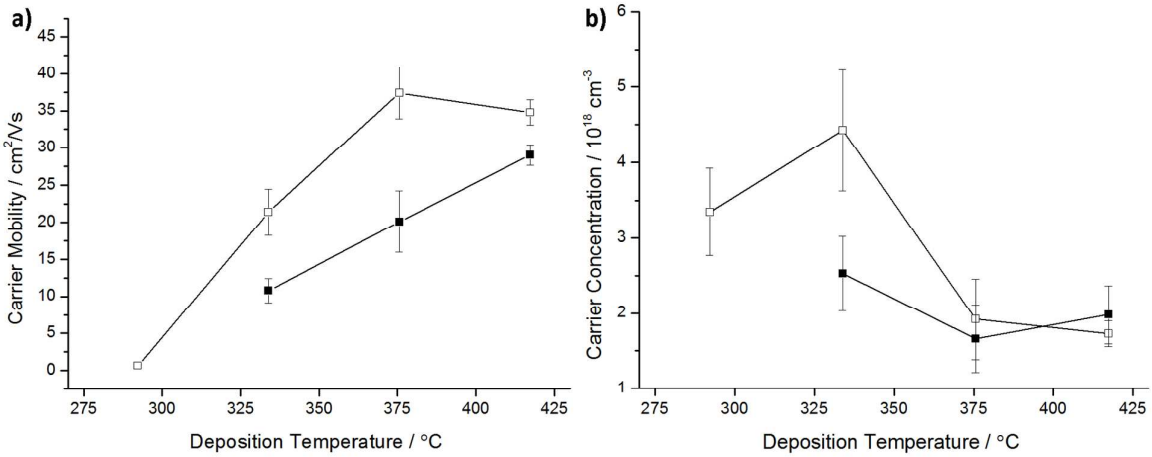

Figure 5 Hall effect a) carrier mobility and b) carrier concentration data as a function of deposition temperature for undoped ZnO films deposited with *in situ* UV irradiation (open symbols) and in the dark (filled symbols), collected without further treatment after sample removal from the deposition chamber.

As will be further discussed, other photoconductive effects are also present in ZnO, including a well-studied "persistent" effect related to the light-induced desorption of air-derived, conductivity-limiting species from ZnO grain boundaries.[24, 25] To minimize the effect of these adsorbed species and to make the new effect under study more apparent, two series of films (with and without *in situ* UV treatment) that had already been exposed to air were then irradiated with UV *ex situ* (Figure 1d). The *ex situ* treatment is intended to remove weakly-adsorbed species from the ZnO grain boundaries,

revealing the electrical properties of the underlying material as a function of *in situ* irradiation and temperature-dependent film microstructure.

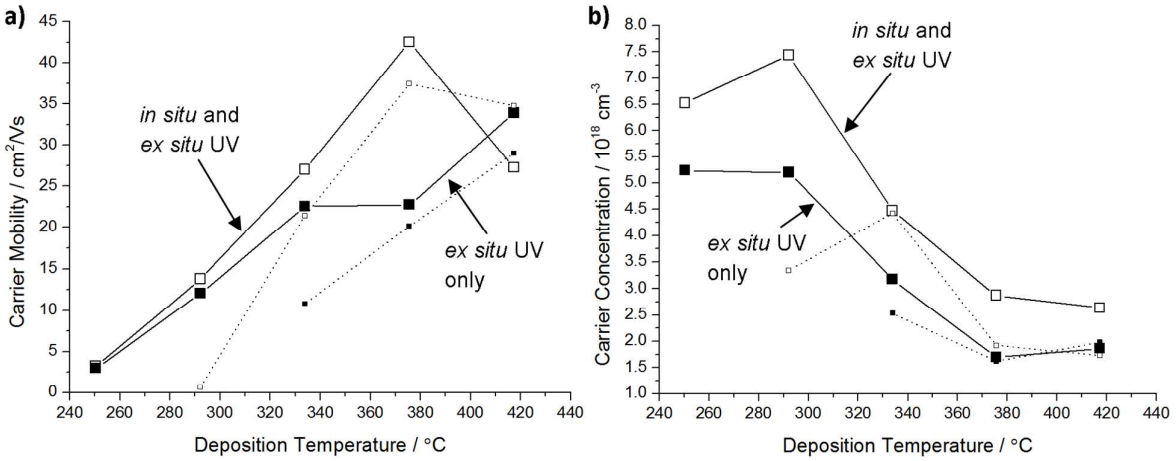

Figure 6 Hall effect a) carrier mobility and b) carrier concentration data as a function of deposition temperature for undoped ZnO films made with *in situ* UV irradiation (open symbols) and in the dark (filled symbols), immediately after an additional *ex situ* irradiation. The corresponding data for the films without *ex situ* UV treatment are also provided on the dotted lines for comparison.

Hall effect mobility and carrier concentration measurements taken immediately after such treatment are displayed in Figures 6a and 6b, respectively. A systematic increase in carrier concentration due to *in situ* irradiation is observed for all deposition temperatures. Additionally, at moderate deposition temperatures (*ca.* 292-376 °C), *in situ* irradiation improves the electron mobility, with the largest relative improvement occurring at a deposition temperature of 376 °C.

The ZnO thin films prepared in this study were also characterized using X-ray diffraction, scanning electron microscopy, UV-Vis-NIR transmission spectrophotometry, and X-ray photoelectron spectroscopy. No structural differences were observed between *in situ* irradiated and dark-deposited films prepared at the same deposition temperature. However, as has been reported elsewhere, there were significant changes in film morphology as a function of deposition temperature.[26, 27]

The X-ray diffraction patterns of all films revealed only one crystalline phase consistent with ZnO in its hexagonal wurtzite form (Figure 7). All films are polycrystalline and composed of crystallites with a preferred orientation relative to the substrate. The degree and direction of orientation depends on the deposition temperature, ranging from almost purely (0 0 2) oriented at high deposition temperatures to a crystallite orientation completely lacking this reflection at low

temperatures. This observation has previously been explained by the fact that growth at the various crystal faces of ZnO have kinetic parameters that vary differently as a function of deposition temperature.[28] While a more or less continuous change in crystalline orientation is observable, the films deposited at 334 °C and above clearly cluster on one side of a morphological transition, while the films deposited at 292 °C and lower are on the other.

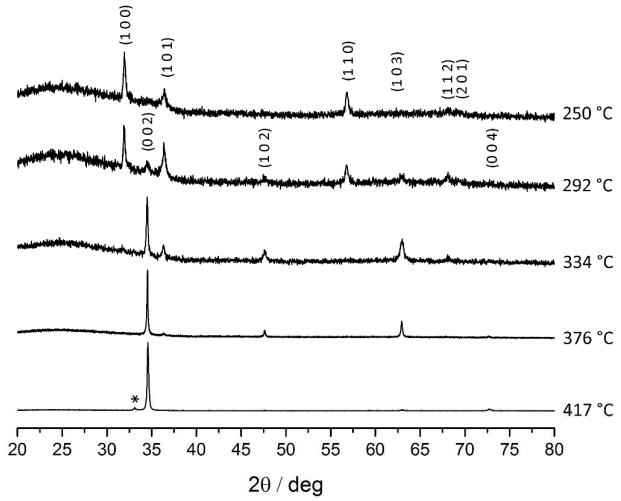

Figure 7 Normalized X-ray diffraction patterns of ZnO thin films deposited at a range of temperatures. The observed peaks are annotated with the corresponding crystalline plane of hexagonal wurtzite ZnO. The minor peak marked with an asterisk * is an instrumental artifact related to tungsten contamination in the Cu x-ray source.

A structural transition with changing deposition temperature is also plainly visible in SEM images (Figure 8). At higher deposition temperatures (*ca.* 376 °C and above) the films consist almost entirely of thin hexagonal platelets stacked mostly parallel to the substrate surface, consistent with the predominance of the (0 0 2) reflection observed by XRD. For the samples deposited at 334 °C, hexagonal platelets are still clearly visible, but they are noticeably less uniform and have an irregular granular material among their stacks. As the deposition temperature is further reduced, a dramatic morphological change again occurs between 334 °C and 292 °C. This temperature range is marked by the complete disappearance of the hexagonal plates and the initial appearance of the feather-like ZnO grains that dominate at low deposition temperatures. The trends seen in SEM also correlate well with the changes observed in the X-ray diffraction patterns of Figure 7.

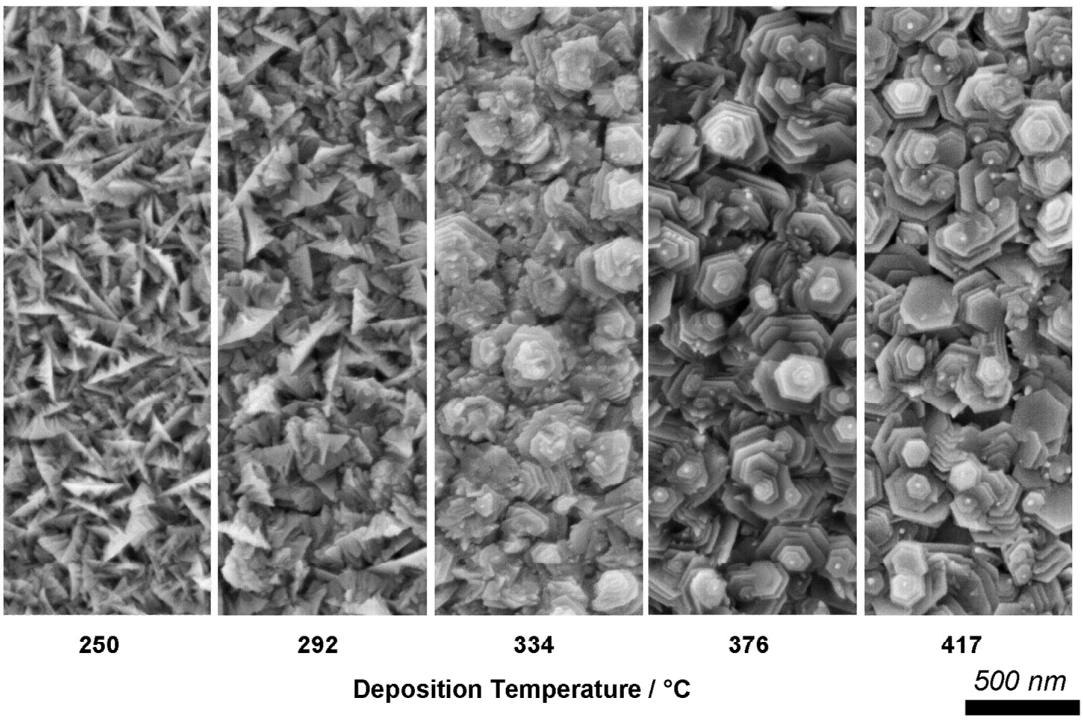

Figure 8 Scanning electron micrographs of undoped ZnO films deposited at a range of substrate temperatures from 250 to 417 °C. A clear change is morphology can be observed across this series, with a particularly sharp change occurring between 292 and 334 °C.

UV-Vis-NIR transmission measurements reveal that film transparency generally increases with decreasing deposition temperature. Once again, a significant change in this parameter occurs between 334 °C and 292 °C. It may additionally be noted that the film thickness deposited per amount of precursor solution per unit time (*i.e.*, the specific deposition rate) also decreases as deposition temperature decreases, though not entirely in concert with the changing visible transparency. These properties, as well as the electrical properties discussed earlier, are summarized in Table 1 for each of the deposition conditions studied.

Table 1 Summary of the properties of ZnO thin films deposited in this study using spray pyrolysis at various deposition temperatures, with and without *in situ* UV irradiation. Where listed, bounds are the standard deviations over a population of samples deposited under those conditions. NM indicates cases where the conductivity is too low for the property to be reliably measured using equipment available. Transmittance data are uncorrected for the glass substrates, which average 92% transparency in the visible range.

T_{dep} / °C		Electron Conc. / 10^{18} cm^{-3}	Mobility / cm^2/Vs	Conductivity / $\Omega^{-1}cm^{-1}$	Est. Thickness / nm	Avg. Visible Trans. / %
417	*Dark*	2.0 ± 0.4	29.0 ± 1.4	8.9 ± 1.4	407 ± 28	70.5 ± 0.5
	UV	1.7 ± 0.2	34.8 ± 1.7	9.5 ± 1.3	396 ± 23	72.7 ± 1.7
376	*Dark*	1.7 ± 0.4	20.1 ± 4.1	4.9 ± 1.5	402 ± 32	74.3 ± 1.4
	UV	1.9 ± 0.5	37.4 ± 3.5	10.6 ± 2.6	388 ± 30	73.3 ± 1.3
334	*Dark*	2.3 ± 0.6	9.8 ± 2.2	3.0 ± 1.5	306 ± 24	72.5 ± 1.1
	UV	4.1 ± 0.7	21.2 ± 2.2	13.3 ± 3.0	299 ± 29	72.8 ± 0.8
292	*Dark*	NM	NM	6.8×10^{-3}	322	79
	UV	3.3 ± 0.6	0.6 ± 0.1	0.3 ± 0.1	255 ± 10	80.5 ± 0.5
250	*Dark*	NM	NM	2.1×10^{-4}	291	87
	UV	NM	NM	8.5×10^{-3}	304	87

Discussion:

From a technological point of view, spray pyrolysis is regarded as a scalable, low-cost, and flexible method for depositing thin films.[8, 29-31] It is notable that this *in situ* UV treatment allows the spray pyrolysis deposition of undoped ZnO films having carrier mobilities similar to those of the best thin films produced by other more complex and capital-intensive techniques, such as vacuum sputtering, pulsed laser deposition, or organometallic chemical vapor deposition.[18] Such mobility values are particularly interesting because the performance of transparent thin film transistors (TFTs) commonly used for active-matrix displays and touchscreens depends explicitly on a semiconducting channel layer with high carrier mobility and low carrier concentration.[32] Combined with an approach for suppressing carrier concentration, our method for producing high mobility, solution-deposited ZnO films may have substantial promise for TFT applications. Work is currently under way to fabricate and characterize TFTs incorporating *in situ* irradiated films.

As would be expected for films deposited by spray pyrolysis, the ZnO films in the present study are polycrystalline, meaning that their macroscopic behavior results from a combination of the distinct properties of both the crystalline ZnO grain interiors and those of the grain boundaries

joining neighboring grains.[21] It is our proposal that the conductivity improvement from *in situ* irradiation results principally from changes in the grain boundary properties, rather than from modification of the ordered bulk regions of the ZnO grains.

Grain boundaries often contain a large population of distorted or dangling bonds, chemisorbed species, and other defects. In the cases typically reported for undoped, as-deposited ZnO, grain boundary defects are dominated by those capable of accepting and trapping electrons from the nearby grain interior.[33] The buildup of negative charge in these surface acceptor states and the corresponding depletion of electrons from the nearby grain interior creates a potential barrier that inhibits electron transport across grain boundaries (Figure 10a).[34] On the other hand, surface donor states, which have, for example, been invoked in films annealed in reducing environments, would produce opposite effects and enhance electrical conductivity.[35-37] When both donors and acceptors are present, their effects can cancel, and it is the excess of one defect type over the other that determines the net overall effect.

The effect of grain boundary potential barriers on the macroscopic electrical properties of thin films can be analyzed by the models of Seto, and Orton and Powell, which treat grain boundaries as back-to-back Schottky barriers in a low voltage regime.[34, 38] Near room temperature, where charge transport over the potential barrier is dominated by thermionic emission, the temperature-dependent Hall mobility is given by:

$$\mu_{Hall} = Le\left(\frac{1}{2\pi m^* kT}\right)^{1/2} exp\left(-\frac{V_b}{kT}\right)$$

where L is an effective grain size, m^* is the electron effective mass, V_b is an activation energy related to the grain boundary barrier height, and k is the Boltzmann constant. When the Hall effect mobilities of films deposited at 376 °C with and without *in situ* UV irradiation were measured as a function of temperature between 80 and 350 K and fitted using this model (Figure 9), the principal difference observed was that films receiving *in situ* UV treatment had a substantially reduced grain boundary potential barrier compared to films deposited in the dark. Notably, the model parameter related to the effective grain size, L, was not significantly changed by the *in situ* irradiation process.

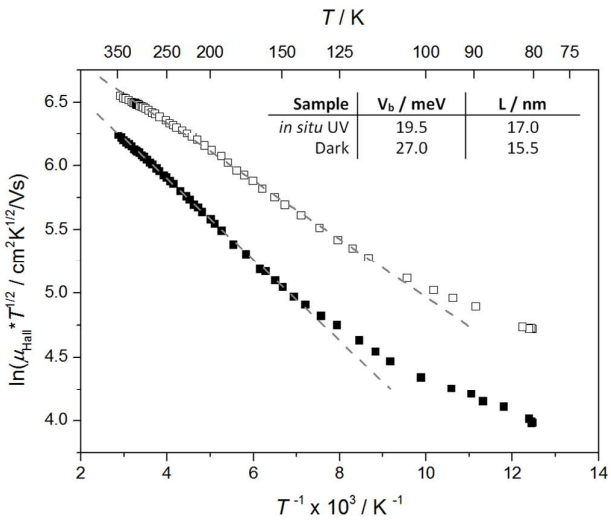

Figure 9 Variable temperature carrier mobility measurements of representative ZnO films deposited at 376 °C with *in situ* irradiation (open symbols) and in the dark (filled symbols). Dashed fit lines to the higher temperature data are shown, as are the grain boundary potential barrier (V_b) and effective grain size (L) extracted from this fit for each sample.

Additionally, the amount of incident UV light required to achieve a conductivity enhancement is small; a radiant flux of less than <150 μW/cm^2 from a handheld UV lamp is enough to produce the significant response observed. We also note that the energy of the photons supplied is substantially lower than the lattice binding energy of crystalline ZnO.[39] Furthermore, a conductivity improvement from *in situ* irradiation still occurs when a film is exposed to UV only at temperatures below 100 °C while cooling under N_2 after deposition. It seems unlikely that such a modest addition of energy at these temperatures would be enough to cause meaningful annealing of the bulk ZnO within the grains, something which normally proceeds appreciably only at a substantial fraction of the melting point (T_m = 1975 °C).[40] That the primary area of effect is the grain boundaries is further corroborated by the sets of structural data obtained by XRD and SEM, neither of which shows any observable difference in gross morphology as a function of film irradiation.

Now working under the hypothesis that *in situ* irradiation affects the grain boundaries of our ZnO thin films, we can consider prior and related work on ZnO photoresponse for insights into the possible origins of the *in situ* UV effect. The effect of radiation on the electrical properties of ZnO has been studied and reported on for nearly 60 years.[25, 41] To date, the aspect of this that has attracted the most attention is the fact that the observed conductivity changes can persist for hours or days

after the irradiation ceases, if the sample is in air. In fact, if a sample is kept under a good vacuum or a rigorously inert atmosphere, the conductivity improvement essentially does not decay.[42]

This phenomenon of so-called *persistent photoconductivity* has been attributed to light-driven changes in the chemical species adsorbed at grain boundaries. It is generally accepted that one or more oxygen-containing moieties derived from the interaction of ZnO surfaces with air are at play, even though the precise roles played by various candidates are not fully resolved. Proposals for relevant species have included chemisorbed O^- and O^{2-},[43] O_2^- and O_2^{2-},[44] as well as CO_2^-.[33] We have also found that "persistent" photoconductivity decays faster when a film is kept under wet nitrogen than when it is kept under dry nitrogen, suggesting that surface hydroxide may also act as an acceptor (Figure 4).

Regardless of their exact origins, the filled, negatively charged acceptor states from such species can attract and be neutralized by the holes generated when ZnO is exposed to light (Figures 10b-c). This reduces the height of the grain boundary potential barriers and has the net effect of increasing the population of conduction band electrons, which both enhance the electrical conductivity of the thin film (Figure 10d). The neutralization of these states also formally represents the breaking of a bond with the ZnO lattice, allowing ready desorption of the formerly chemisorbed species.[24, 33] When irradiation ceases with the sample in air, the grain boundary speciation returns to its pre-irradiation state over the course of hours (or days) as components of the atmosphere re-adsorb and reform electron-accepting defects. Thus, while the oft-reported photoconductivity in ZnO is called "persistent" because equilibrium is achieved via a relatively slow chemical process as opposed to a fast electronic one, it is nevertheless unstable under ambient conditions.

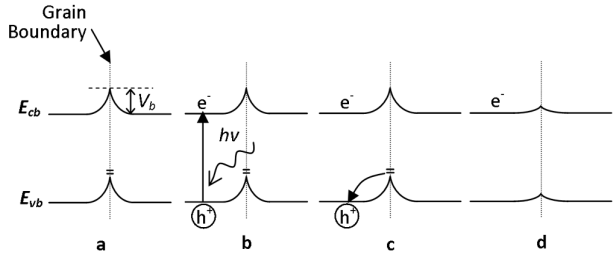

Figure 10 General schematic of changes in the near grain boundary band structure of ZnO with surface acceptors upon UV irradiation. Neutralization of filled acceptor states at the grain boundary by photogenerated holes results in increases in both carrier concentration and mobility.

In stark contrast, we have discovered that the conductivity enhancement resulting from *in situ* UV treatment appears to be much longer lasting. Nevertheless, our view is that the general principles behind "persistent" photoconductivity can still be applied, as *any* change in grain boundary chemistry that reduces the net density of surface acceptor states would cause a concurrent increase in carrier mobility and concentration (Figure 10). This can occur either by removal of acceptors or by the formation of compensating donors. How long the resulting conductivity increase persists depends on the extent and/or rate of any reverse process that may occur when illumination ceases.

Thus, the *in situ* UV effect can be accounted for by (meta)stable, light-induced surface donors that can only form before a recently deposited sample is exposed to air. On the other hand, "persistent" photoconductivity is related to the reversible desorption of weakly bound chemical species introduced by air exposure. Figure 6 shows that the effects of *in situ* irradiation and those of "persistent" photoconductivity can be observed simultaneously, implying that more than one process or species is acting to modify the donor/acceptor density at the ZnO grain boundaries. While there is presently not enough information to make definitive atom-level mechanistic proposals, it is possible to suggest reasonable systems that fit these qualitative constraints.

For instance, theoretical calculations indicate that an oxygen-deficient ZnO surface would lead to the presence of surface donor states.[45] Under oxygen-poor, slightly reducing conditions (as in a N_2-filled deposition chamber) the loss of near-surface lattice oxygen to form vacancies (V_O) is only slightly disfavored at thermal equilibrium, suggesting that a substantive population of surface V_O could be formed under the hole-rich conditions of UV irradiation. Such states have also been proposed based on experimental studies of the irradiation of ZnO under high vacuum.[39] Our observation that *in situ* UV treatment is most effective when ZnO films are cooled to room temperature under irradiation is consistent with the expectation that defect-neutralizing reactions are most facile at higher temperatures. In effect, irradiation as a film cools causes a metastable surface V_O population to be frozen in. For *in situ* treated films, this enhanced population of surface donors

can partially compensate for the acceptors that form upon subsequent air exposure, leading to a smaller excess of surface acceptors and a higher electrical conductivity.

For further insight, we may consider the oxygen 1s XPS spectra of films deposited at low deposition temperature (292 °C) with *in situ* irradiation (Figure 11a) and in the dark (Figure 11b), where the effects of *in situ* irradiation are most apparent. As has previously been reported, these experimental spectra can be deconvoluted into three components, centered at approximately 530.5, 531.8, 532.7 eV.[46, 47] Compared to deposition in the dark, *in situ* irradiation clearly causes the intensity of the highest binding energy component at ~532.7 eV to be reduced relative to that of the largest component at ~530.5 eV. A similar, but much less dramatic effect is observed when *in situ* irradiation is applied at higher deposition temperatures.

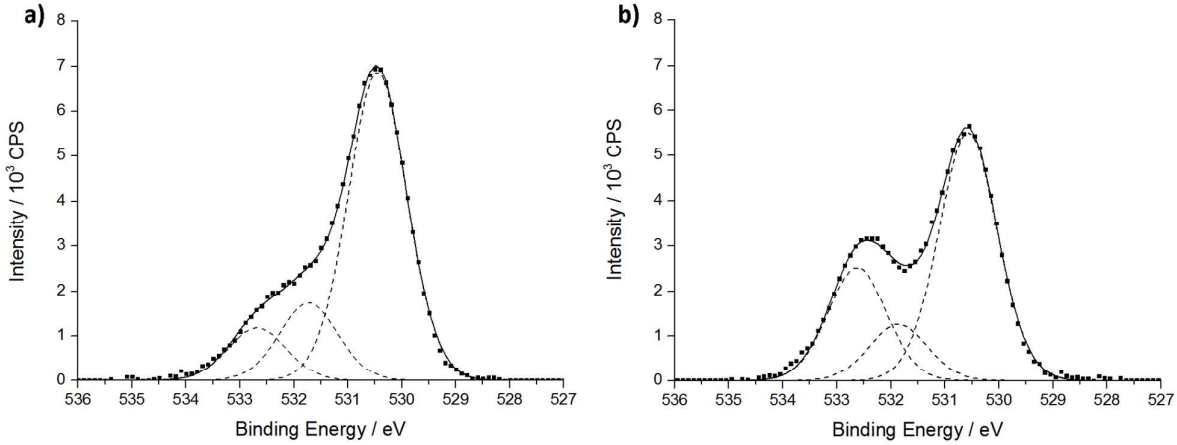

Figure 11 Experimental O(1s) x-ray photoelectron spectra for ZnO thin films deposited at a substrate temperature of 292 °C with a) *in situ* UV irradiation and b) in the dark (square symbols). The fit to each set of experimental data (solid line) consists of 3 components (dashed lines) centered at binding energies of approximately 530.5, 531.8, and 532.7 eV.

It is relatively uncontroversial that the largest and lowest binding energy component centered at ~530.5 eV corresponds to the oxide ions of the ordered ZnO lattice.[48] More controversy surrounds assignment of the components at higher binding energy, which is complicated by the fact many non-metal oxide species possess similar binding energies in this range. It should also be noted that the fitting of three components is not unique, and that it cannot be determined from these data alone whether exactly 3 or more components are contributing to the observed lineshape. With these caveats in mind, the middle component centered at ~531.8 eV has previously been linked to oxygen in locally oxygen-deficient regions,[49, 50] while the higher energy component centered at ~532.7 eV has

been attributed to a variety of surface-adsorbed oxygen-containing species, such as hydroxides and carbonates.[47, 51, 52] While it has been demonstrated that the XPS signal for chemically-bound surface carbonate appears in this region of the O(1s) spectrum, we tend to discount changes in carbon as a major factor in the present system, as no significant changes were observed in the corresponding C(1s) XPS spectra as a function of *in situ* irradiation.[53, 54]

Li, *et al*. have suggested that surface hydroxide binds to a ZnO (0 0 2) surface in different modes depending on the types and concentrations of surface defects present.[45] Other workers have used thermal desorption measurements to experimentally distinguish various oxygen-containing species that bind to the ZnO surface with differing strengths.[17, 44, 55] For instance, it is conceivable that air-derived species like hydroxide may either be loosely adsorbed (contributing to the highest energy XPS component), or bind more stably, say, by replacing the missing oxygen from a surface V_O (contributing to the main oxide XPS signal). Given this interpretation, the apparent reduction in intensity of the highest binding energy O(1s) XPS component is consistent with a more oxygen deficient underlying surface that we suggest arises due to *in situ* UV irradiation.

Under the oxygen-rich conditions after air exposure, surface donor formation by removal of oxygen from the ZnO lattice is highly unfavorable. In such a case, irradiation only induces desorption of less strongly bound species, giving rise to classic "persistent" photoconductivity, but not an effect comparable to *in situ* irradiation. The possibility that air-derived species may bind by filling a surface V_O may also be invoked to explain why the effect of *in situ* irradiation cannot be achieved by UV treatment after returning a sample to inert atmosphere. It has been reported that the stability afforded by nearly stoichiometric ZnO raises the formation energy for defects.[56] Since the removal of surfaces vacancies by air exposure locally reduces non-stoichiometry, the likelihood of further V_O formation is thus decreased.

Consideration of how these photoconductive effects vary as a function of deposition temperature allows an essential link to be made between these microscopic phenomena and the challenges facing ZnO thin films as practical engineering materials. When the deposition

temperature is reduced below ~334 °C, say, into a range that is comfortably compatible with inexpensive polymer substrates, the effect of weakly adsorbed species becomes the primary factor limiting electronic conduction. The ZnO films prepared at the lowest deposition temperatures have *as deposited* electrical conductivities many (at least 4-5) orders of magnitude lower than those deposited above 334 °C. However, when the effect of air-derived grain boundary acceptors is temporarily relieved by *ex situ* irradiation (Figure 1d), all films in the present study deposited at 292 °C and above only differ in electrical conductivity by at most a few tens of percent. After this treatment, even the film deposited below the reported onset temperature of zinc acetate decomposition (~251 °C) and likely suffering from incomplete decomposition of the precursor was only 5.5 times more resistive than its higher temperature counterparts.[57]

At least qualitatively, both the trends in *as deposited* electrical conductivity and the magnitude of *ex situ* photoresponse correlate extremely well with the changes in film morphology that occur as a function of deposition temperature. These electrical properties show a sharp change around a deposition temperature of 334 °C, near where the film morphology transitions from the hexagonal platelets characteristic of high deposition temperatures to the feather-like low temperature structure (Figure 8). The appearance of the ZnO grains in the low deposition temperature films suggests that they have more surface area (possibly with a different distribution of exposed crystallographic faces or surface defects) upon which atmospheric species may adsorb and form acceptor states. In other words, even though *in situ* treatment appears effective at all deposition temperatures, for lower temperature films, its effect is overwhelmed by the larger number of acceptor states that can form when these films are exposed to air.

Thus, we have demonstrated here that *in situ* UV irradiation represents a useful way to significantly improve the electrical properties of ZnO films prepared at moderate temperatures, and that the challenge of producing stable, highly conductive ZnO thin films at lower temperatures lies in the understanding and mitigation of air-dependent grain boundary effects.

Conclusion:

A new *in situ* UV irradiation treatment of thin film ZnO samples under a nitrogen atmosphere has been shown to produce a substantial and long-lasting improvement in electrical conductivity relative to the same films deposited in the dark. Using spray pyrolysis at moderate deposition temperatures (334-417 °C), ZnO thin films can be produced with record carrier mobilities as high as 44.3 cm^2/Vs, which may be of significant interest for applications in transparent thin film transistors. This treatment also effectively lowers the deposition temperature required to deposit the highest conductivity ZnO films.

It has also been shown that this new *in situ* irradiation effect operates in addition to and largely independent of classic "persistent" photoconductivity. While both of these processes influence electronic transport by modifying the defect density at ZnO grain boundaries, their ability to do so is affected differently by deposition temperature-dependent changes in film microstructure. Our observations suggest that the air-derived species at play in "persistent" photoconductivity are the primary limiter of conductivity at low deposition temperatures. This should be the area of focus in continuing efforts to reduce the temperatures required to deposit highly conductive ZnO films.

While the theoretical understanding of idealized, single crystal semiconductors has progressed dramatically in recent years, the results presented here highlight the overriding importance of grain boundary effects in determining the electrical properties of polycrystalline transparent conducting films. There is little doubt that an unravelling of the complex and interconnected processes occurring at grain boundaries is a substantial endeavor. Nevertheless, we hope to have shown that new and important insights about this problem can still be found, even by using time-honored approaches such as the exposure of transparent conducting films to UV light, both as a processing technique and as a method for probing fundamental questions about electron transport in these materials.

Acknowledgements:

The authors gratefully acknowledge support from the Clarendon Scholarship Fund and from Ms. Nazanin Rashidi and Dr. Michael Jones for many useful discussions and guidance. We are also indebted to Dr. Jose Portoles for the collection of X-ray photoelectron spectra at the National EPSRC XPS User's Service (NEXUS) at Newcastle University.

References:

1 D. Ginley, H. Hosono and D. C. Paine, *Handbook of Transparent Conductors*, Springer, New York, 2011.

2 B. G. Lewis and D. C. Paine, *MRS Bull.,* 2000, **25**, 22-27.

3 K. Ghaffarzadeh and R. Das, *Transparent Conductive Films (TCF) 2013-2023: Forecasts, Technologies, and Players*, IdTechEx, Cambridge, UK, 2013.

4 P. P. Edwards, A. Porch, M. O. Jones, D. V. Morgan and R. M. Perks, *Dalton Trans.,* 2004, **19**, 2995-3002.

5 R. G. Gordon, *MRS Bull.,* 2000, **25**, 52-57.

6 S. Major, A. Banerjee and K. L. Chopra, *Thin Solid Films,* 1983, **108**, 333-340.

7 N. Rashidi, V. L. Kuznetsov, J. R. Dilworth, M. Pepper, P. J. Dobson and P. P. Edwards, *J. Mater. Chem. C,* 2013, **1**, 6960-6969.

8 J. B. Mooney and S. B. Radding, *Ann. Rev. Mater. Sci.,* 1982, **12**, 81-101.

9 C. W. Litton, D. C. Reynolds and T. C. Collins, *Zinc Oxide Materials for Electronic and Optoelectronic Device Applications*, Wiley, Chichester, UK, 2011.

10 C. F. Klingshirn, A. Waag, A. Hoffmann and J. Geurts, *Zinc Oxide: From Fundamental Properties Towards Novel Applications*, Springer, Heidelberg, Germany, 2010.

11 Z. C. Feng, *Handbook of Zinc Oxide and Related Materials*, CRC Press, Boca Raton, FL, 2012.

12 J. Suehiro, N. Nakagawa, S. Hidaka, M. Ueda, K. Imasaka, M. Higashihata, T. Okada and M. Hara, *Nanotechnology,* 2006, **17**, 2567-2573.

13 Q. Wan, Q. H. Li, Y. J. Chen, T. H. Wang, X. L. He, J. P. Li and C. L. Lin, *Appl. Phys. Lett.,* 2004, **84**, 3654-3656.

14 R. Martins, E. Fortunato, P. Nunes, I. Ferreira, A. Marques, M. Bender, N. Katsarakis, V. Cimalla and G. Kiriakidis, *J. Appl. Phys.,* 2004, **96**, 1398-1408.

15 R. Barnes, R. Molina, J. Xu, P. Dobson and I. Thompson, *J. Nanopart. Res.,* 2013, **15**, 1-11.

16 A. Mclaren, T. Valdes-Solis, G. Li and S. C. Tsang, *J. Am. Chem. Soc.,* 2009, **131**, 12540-12541.

17 E. Molinari, F. Cramarossa and F. Paniccia, *J. Catal.,* 1965, **4**, 415-429.

18 K. Ellmer, *J. Phys. D,* 2001, **34**, 3097-3108.

19 A. Salleo and W. S. Wong, *Flexible Electronics: Materials and Applications*, Springer, New York, NY, 2009.

20 W. A. MacDonald, *J. Mater. Chem.,* 2004, **14**, 4-10.

21 A. T. Vai, V. L. Kuznetsov, H. Jain, D. Slocombe, N. Rashidi, M. Pepper and P. P. Edwards, *Z. Anorg. Allg. Chem.,* 2014, **640**, 1054-1062.

22 L. J. van der Pauw, *Philips Tech. Rev.,* 1958, **20**, 220-224.

23 R. Swanepoel, *J. Phys. E Sci. Instrum.,* 1983, **16**, 1214-1222.

24 D. B. Medved, *J. Chem. Phys.,* 1958, **28**, 870-873.

25 D. A. Melnick, *J. Chem. Phys.,* 1957, **26**, 1136-1146.

26 D. F. Paraguay, L. W. Estrada, N. D. R. Acosta, E. Andrade and M. Miki-Yoshida, *Thin Solid Films,* 1999, **350**, 192-202.

27 J. L. van Heerden and R. Swanepoel, *Thin Solid Films,* 1997, **299**, 72-77.

28 Z. L. Wang, *J. Phys.-Condens. Mat.,* 2004, **16**, R829-R858.

29 M. S. Tomar and F. J. Garcia, *Prog. Cryst. Growth Ch.,* 1981, **4**, 221-248.

30 B. R. Pamplin, *Prog. Cryst. Growth Ch.,* 1979, **1**, 395-403.

31 P. S. Patil, *Mater. Chem. Phys.,* 1999, **59**, 185-198.

32 S. Jeong and J. Moon, *J. Mater. Chem.,* 2012, **22**, 1243-1250.

33 Y. Shapira, R. B. McQuistan and D. Lichtman, *Phys. Rev. B,* 1977, **15**, 2163-2169.

34 J. W. Orton and M. J. Powell, *Rep. Prog. Phys.,* 1980, **43**, 1263-1307.

35 R. J. Collins and D. G. Thomas, *Phys. Rev.,* 1958, **112**, 388-395.

36 G. Heiland, *Z. Physik,* 1957, **148**, 15-27.

37 G. Heiland, *Z. Physik,* 1957, **148**, 28-33.

38 J. Y. W. Seto, *J. Appl. Phys.,* 1975, **46**, 5247-5254.

39 R. Gurwitz, R. Cohen and I. Shalish, *J. Appl. Phys.,* 2014, **115**, 033701.

40 H. Ko, M. Han, Y. Park, Y. Yu, B. Kim, S. S. Kim and J. Kim, *J. Cryst. Growth,* 2004, **269**, 493-498.

41 E. Mollwo, in *Photoconductivity Conference*, ed. R. G. Breckendridge, B. R. Russell and E. E. Hahn, John Wiley and Sons, New York, 1954, p. 509.

42 G. Heiland, *J. Phys. Chem. Solids,* 1961, **22**, 227-234.

43 J. Bao, I. Shalish, Z. Su, R. Gurwitz, F. Capasso, X. Wang and Z. Ren, *Nanoscale Res. Lett.,* 2011, **6**, 404-410.

44 T. I. Barry and F. S. Stone, *P. Roy. Soc. Lond. A Mat.,* 1960, **255**, 124-144.

45 H. Li, L. K. Schirra, J. Shim, H. Cheun, B. Kippelen, O. L. A. Monti and J. Bredas, *Chem. Mater.,* 2012, **24**, 3044-3055.

46 S. Park, T. Ikegami and K. Ebihara, *Thin Solid Films,* 2006, **513**, 90-94.

47 S. Lee, S. Bang, J. Park, S. Park, W. Jeong and H. Jeon, *physica status solidi (a),* 2010, **207**, 1845-1849.

48 B. J. Coppa, R. F. Davis and R. J. Nemanich, *Appl. Phys. Lett.,* 2003, **82**, 400-402.

49 J. C. C. Fan and J. B. Goodenough, *J. Appl. Phys.,* 1977, **48**, 3524-3531.

50 D. E. Pugel, R. D. Vispute, S. S. Hullavarad, T. Venkatesan and B. Varughese, *Appl. Surf. Sci.,* 2008, **254**, 2220-2223.

51 T. L. Barr, *J. Phys. Chem.,* 1978, **82**, 1801-1810.

52 S. Major, S. Kumar, M. Bhatnagar and K. L. Chopra, *Appl. Phys. Lett.,* 1986, **49**, 394-396.

53 C. T. Au, W. Hirsch and W. Hirschwald, *Surf. Sci.,* 1988, **199**, 507-517.

54 C. T. Au, W. Hirsch and W. Hirschwald, *Surf. Sci.,* 1988, **197**, 391-401.

55 A. M. Peers, *J. Phys. Chem.,* 1963, **67**, 2228-2229.

56 S. A. Studenikin, N. Golego and M. Cocivera, *J. Appl. Phys.,* 1998, **84**, 2287-2294.

57 T. Arii and A. Kishi, *Thermochim. Acta,* 2003, **400**, 175-185.

A new *in situ* approach for treating polycrystalline zinc oxide thin film transparent conductors with UV light under a slightly reducing nitrogen atmosphere results in a long-lasting improvement in electrical properties and provides insights into the mechanisms that limit electronic conductivity in these materials.

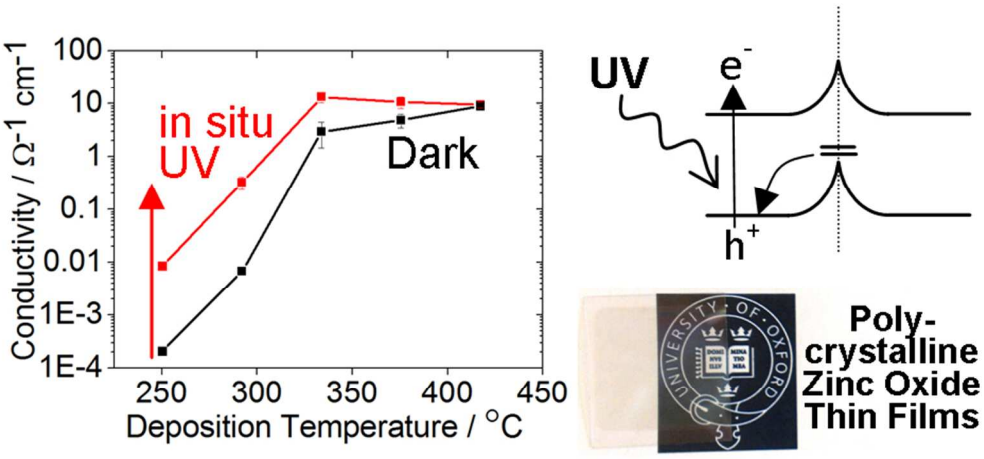

80x39mm (300 x 300 DPI)